# Feedback stabilization of resistive shell modes in a reversed field pinch

R. Fitzpatrick and E.P. Yu
*Institute for Fusion Studies*
*Department of Physics*
*University of Texas at Austin*
(October 27, 1998)

A reactor relevant reversed field pinch (RFP) must be capable of operating successfully when surrounded by a close-fitting resistive shell whose L/R time is much *shorter* than the pulse length. Resonant modes are largely unaffected by the resistivity of the shell, provided that the plasma rotation is maintained against the breaking effect of non-axisymmetric eddy currents induced in the shell. This may require an auxiliary momentum source, such as a neutral beam injector. Non-resonant modes are largely unaffected by plasma rotation, and are expected to manifest themselves as non-rotating *resistive shell modes* growing on the L/R time of the shell. A general RFP equilibrium is subject to many simultaneously unstable resistive shell modes. The only viable control mechanism for resistive shell modes in an RFP reactor is *active feedback*.

It is demonstrated that an $N$-fold toroidally symmetric arrangement of feedback coils, combined with a strictly linear feedback algorithm, is capable of *simultaneously stabilizing* all intrinsically unstable resistive shell modes over a wide range of different RFP equilibria. The number of coils in the toroidal direction $N$ must be greater than, or equal to, the range of toroidal mode numbers of the unstable resistive shell modes. However, this range is largely determined by the aspect-ratio of the device. The optimum coil configuration corresponds to one in which each feedback coil overlaps its immediate neighbours in the toroidal direction. The critical current which must be driven around each feedback coils is, at most, a few percent of the equilibrium toroidal plasma current. The feedback scheme is robust to small deviations from pure $N$-fold toroidal symmetry or a pure linear response of the feedback circuits.

## I. INTRODUCTION

A reversed field pinch (or RFP) is a magnetic fusion device which is similar to a tokamak [1] in many ways. Like a tokamak, the plasma is confined by a combination of a toroidal magnetic field, $B_\phi$, and a poloidal magnetic field, $B_\theta$, in an axisymmetric toroidal configuration [2]. Unlike a tokamak, where $B_\phi \gg B_\theta$, the toroidal and poloidal field-strengths are comparable, and the RFP toroidal field is largely generated by currents flowing within the plasma. The RFP concept derives its name from the fact that the direction of the toroidal field is reversed (compared to the direction of the externally generated toroidal field) in the outer regions of the plasma. This reversal is a consequence of relaxation to a minimum energy state driven by intense magnetohydrodynamical (MHD) mode activity during the plasma start-up phase [3]. Constant low-level mode activity maintains the reversal, by dynamo action, throughout the duration of the plasma discharge. As a magnetic fusion concept, the RFP has a number of possible advantages relative to the tokamak. The magnetic field-strength at the coils is relatively low, allowing the possibility of a copper-coil, as opposed to a super-conducting-coil, reactor. Furthermore, the plasma current can, in principle, be increased sufficiently to allow ohmic ignition, thus negating the need for auxiliary heating systems.

A general MHD instability in an RFP is characterized by its poloidal mode-number $m$ and its toroidal mode-number $n$. These integers represent the number of periods in the poloidal and toroidal directions, respectively. In this paper, the convention is adopted that $m \geq 0$, whereas $n$ may take any integer value. The MHD instabilities of an RFP plasma are conventionally separated into *five* distinct groups. The $m = 0$ modes are resonant at the *reversal surface*, where the equilibrium toroidal magnetic field reverses sign (see Fig. 1). Note that a *resonant* mode is one that satisfies $\boldsymbol{k}\cdot\boldsymbol{B} = 0$ somewhere inside the plasma, where $\boldsymbol{k}$ is the wave-vector of the mode and $\boldsymbol{B}$ is the equilibrium magnetic field. The remaining four groups consist of $m = 1$ modes. *Internally resonant* modes are $n > 0$ modes resonant inside the reversal surface (where $B_\phi$ has the same sign as $B_\theta$). *Externally resonant* modes are $n < 0$ modes resonant outside the reversal surface (where $B_\phi$ has the opposite sign as $B_\theta$). *Internally non-resonant* modes are $n > 0$ non-resonant modes which have a similar helicity to the equilibrium magnetic field close to the magnetic axis. Finally, *externally non-resonant* modes are $n < 0$ non-resonant modes which have a similar helicity to the equilibrium magnetic field outside the plasma boundary.

A conventional RFP plasma is surrounded by a close-fitting *perfectly conducting* shell: *i.e.*, a shell whose L/R time is much *longer* than the pulse length of the plasma discharge. Such a shell generally stabilizes the $m = 0$ modes, the internally and externally non-resonant modes, and the externally resonant modes [4–6]. The internally resonant modes remain unstable, and are responsible for the dynamo action which maintains the RFP discharge against ohmic decay [7]. Consequently, the internally resonant modes are often referred to as *dynamo modes*.

A realizable RFP reactor is bound to have a pulse length which is considerably longer than the L/R time of any conceivable shell surrounding the plasma. Thus, before the RFP concept can be considered to be a serious alternative to the tokamak concept, as a fusion energy source, it is necessary to demonstrate that an RFP can operate successfully when surrounded by a close-fitting *resistive shell*: *i.e.*, a shell whose L/R time is much *shorter* than the pulse length of the plasma discharge.

Consider the effect of a close-fitting resistive shell on the five previously mentioned classes of MHD instabilities. As is well-known, a *resonant* mode (*i.e.*, an $m = 0$ mode, or an internally or externally resonant mode) is convected by the plasma at its associated *rational surface* (*i.e.*, the flux-surface where $\boldsymbol{k}\cdot\boldsymbol{B} = 0$). Since an RFP plasma generally rotates in the laboratory frame, it follows that resonant modes are usually *rotating* modes. If the typical plasma rotation rate greatly exceeds the inverse L/R time of the shell, as is invariably the case, then the resistive shell behaves effectively as an ideal shell as far as the rotating modes are concerned. It follows that the stability of resonant modes is largely unaffected by the resistivity of the shell [6]. Thus, the dynamo modes are expected to be the only intrinsically unstable resonant modes in a rotating RFP plasma surrounded by a close-fitting resistive shell.

It should be noted that a resistive shell exerts a non-linear, inductive, slowing-down torque on any rotating dynamo modes in the plasma [8]. In fact, if the amplitude of the dynamo modes becomes sufficiently large, this torque can *arrest* the plasma rotation [9,10], in which case *all* resonant modes unstable in the absence of a shell are expected to grow on the L/R time of the shell [11–14]. In other words, a resistive shell is incapable of stabilizing *any* modes in the absence of plasma rotation. In this paper, it is assumed that either the amplitude of the dynamo modes never gets sufficiently high to arrest the plasma rotation, or, alternatively, that the RFP is equipped with an auxiliary momentum source (*e.g.*, a neutral beam injector) which is capable of maintaining the plasma rotation in the presence of the non-linear slowing-down torques due to the shell. Either way, the resistive shell is assumed to act like an ideal shell as far as the resonant modes are concerned.

Unfortunately, the stability of internally and externally non-resonant modes in RFPs *is not* affected by plasma rotation, except in the extremely unlikely event that the rotation velocity becomes comparable with the Alfvén velocity [15]. Thus, a rotating RFP plasma surrounded by a close-fitting resistive shell is expected to be unstable to non-rotating, internally and externally non-resonant modes, growing on the L/R time of the shell, in addition to the ever-present, rotating dynamo modes. These non-rotating modes are referred to collectively as *resistive shell modes*.

The experimental data-base regarding the effect of resistive shell modes on RFP discharges is highly incomplete, since the only RFP experiments equipped with shells suitable for investigating these modes (*i.e.*, OHTE [16], HBTX-1C [17], Extrap-T1 [18], and Reversatron-II [19]) were all terminated prematurely for fiscal reasons. Hopefully, the newly commissioned Extrap-T2 [20] device will shortly provide some much needed additional data. Nevertheless, there exists good evidence from HBTX-1C [17] that resistive shell modes (*i.e.*, non-rotating, *non-resonant* modes growing on the L/R time of the shell) are present in an RFP surrounded by a resistive shell, and have a highly detrimental effect on the plasma discharge. This strongly suggests that resistive shell modes will need to be stabilized in an RFP reactor. (Inexplicably, resistive shell modes were not observed on the OHTE[16] device. Nevertheless, in this paper, in the absence of any cogent arguments demonstrating that RFP reactors should behave like OHTE, rather than HBTX-1C, the conservative assumption is made that resistive shell modes are likely to be unstable in a reactor).

Given that resistive shell modes must be stabilized in an RFP reactor, and that this stabilization cannot be achieved via any realizable level of plasma rotation, the only remaining viable option is to stabilize the modes by some sort of active feedback [21]. It should be noted that resistive shell modes are also predicted to be a problem in "advanced" tokamak reactors, and that active feedback has been proposed as a solution in this case as well [22–24]. In tokamaks, there is generally only a *single* intrinsically unstable resistive shell mode at any given time, which renders the design of a practical feedback scheme relatively straightforward [24]. In RFPs, on the other hand, there are generally *multiple* intrinsically unstable resistive shell modes at any given time. Thus, in an RFP, a successful feedback scheme must be capable of *simultaneously* stabilizing many independent resistive shell modes of different helicities. Clearly, the feedback stabilization of resistive shell modes is a far more difficult prospect in RFPs than in tokamaks.

The feedback stabilization of strongly coupled dynamo and resistive shell modes in a non-rotating RFP plasma was very briefly investigated in HBTX-1C [25], and was later simulated using a 3-D non-linear MHD code [26]. This is a somewhat different, and considerably more difficult, problem to that studied here.

In summary, the aim of this paper is to investigate the feasibility of the simultaneous feedback stabilization of *all* intrinsically unstable resistive shell modes in a *rotating* RFP plasma surrounded by a close-fitting, thin resistive shell.

## II. PRELIMINARY ANALYSIS

### A. The plasma equilibrium

Consider a large aspect-ratio[27], zero-$\beta$[28], RFP plasma equilibrium whose unperturbed magnetic flux-surfaces map out (almost) concentric circles in the poloidal plane. Such an equilibrium is well approximated as a periodic cylinder. Suppose that the minor radius of the plasma is $a$. Standard cylindrical polar coordinates $(r,\theta,z)$ are adopted. The system is assumed to be periodic in the $z$-direction, with periodicity length $2\pi R_0$, where $R_0$ is the simulated major radius of the plasma. It is convenient to define a simulated toroidal angle $\phi = z/R_0$.

The equilibrium magnetic field is written

$$\boldsymbol{B} = [0, B_\theta(r), B_\phi(r)]\,. \tag{1}$$

The model RFP equilibrium adopted in this paper is the well-known $\alpha$–$\Theta_0$ model[29], according to which

$$\nabla\wedge\boldsymbol{B} = \sigma(r)\,\boldsymbol{B}, \tag{2}$$

where

$$\sigma = \left(\frac{2\,\Theta_0}{a}\right)\left[1-\left(\frac{r}{a}\right)^\alpha\right]. \tag{3}$$

Here, $\Theta_0$ and $\alpha$ are positive constants.

It is conventional[2] to parameterize RFP equilibria in terms of the *pinch parameter*,

$$\Theta = \frac{B_\theta(a)}{\langle B_\phi\rangle}, \tag{4}$$

and the *reversal parameter*,

$$F = \frac{B_\phi(a)}{\langle B_\phi\rangle}, \tag{5}$$

where $\langle\cdots\rangle$ denotes a volume average.

### B. The perturbed magnetic field

In the following, all perturbed quantities are tacitly assumed to possess a common $\exp(\gamma\,t)$ time dependence. The magnetic perturbation associated with a general resistive instability can be written

$$\boldsymbol{b}(\boldsymbol{r}) = \sum_{m,n}\boldsymbol{b}^{m,n}(r)\,\mathrm{e}^{\,\mathrm{i}\,(m\,\theta-n\,\phi)}, \tag{6}$$

where

$$b_r^{m,n} = \frac{\mathrm{i}\,\psi^{m,n}}{r}, \tag{7}$$

$$b_\theta^{m,n} = -\frac{m\,(\psi^{m,n})'}{m^2+n^2\epsilon^2} + \frac{n\epsilon\,\sigma\,\psi^{m,n}}{m^2+n^2\epsilon^2}, \tag{8}$$

$$b_\phi^{m,n} = \frac{n\epsilon\,(\psi^{m,n})'}{m^2+n^2\epsilon^2} + \frac{m\,\sigma\,\psi^{m,n}}{m^2+n^2\epsilon^2}. \tag{9}$$

Here, $'$ denotes $d/dr$. Furthermore,

$$\epsilon(r) = \frac{r}{R_0}. \tag{10}$$

The linearized magnetic flux function $\psi^{m,n}(r)$ satisfies Newcomb's equation[30],

$$\frac{d}{dr}\left[f^{m,n}\,\frac{d\psi^{m,n}}{dr}\right]-g^{m,n}\,\psi^{m,n}=0, \tag{11}$$

where

$$f^{m,n}(r)=\frac{r}{m^2+n^2\epsilon^2}, \tag{12}$$

$$g^{m,n}(r)=\frac{1}{r}+\frac{r\,(n\epsilon\,B_\theta+m\,B_\phi)}{(m^2+n^2\epsilon^2)(m\,B_\theta-n\epsilon\,B_\phi)}\,\frac{d\sigma}{dr}+\frac{2\,m\,n\epsilon\,\sigma}{(m^2+n^2\epsilon^2)^2}-\frac{r\,\sigma^2}{m^2+n^2\epsilon^2}. \tag{13}$$

In the vacuum region ($\sigma=0$) surrounding the plasma, the most general solution to Newcomb's equation takes the form

$$\psi^{m,n}=A\,i_m(n\epsilon)+B\,k_m(n\epsilon), \tag{14}$$

where $A,B$ are arbitrary constants, and

$$i_m(n\epsilon)=|n\epsilon|\,I_{m+1}(|n\epsilon|)+m\,I_m(|n\epsilon|), \tag{15}$$

$$k_m(n\epsilon)=-|n\epsilon|\,K_{m+1}(|n\epsilon|)+m\,K_m(|n\epsilon|). \tag{16}$$

Here, $I_m,K_m$ represent standard modified Bessel functions. For the special case $n=0$, the most general vacuum solution is written

$$\psi^{m,0}=A\,\epsilon^m+B\,\epsilon^{-m}. \tag{17}$$

### C. Shell physics

Suppose that the plasma is surrounded by a uniform, thin, rigid, concentric, conducting shell of minor radius $r_w$, radial thickness $\delta_w$, and conductivity $\sigma_w$. The L/R time, or *time constant*, of the shell is defined

$$\tau_w=\mu_0\,\sigma_w\,\delta_w\,r_w. \tag{18}$$

All analysis in this paper is performed in the *thin shell* limit, in which the skin depth of the perturbed magnetic field in the shell material is much greater than the thickness of the shell, but much less than its radius. In this limit, there is negligible radial variation of the perturbed magnetic field and the eddy current density across the shell. The thin shell limit is valid whenever

$$\frac{\delta_w}{r_w}\ll|\gamma|\tau_w\ll\frac{r_w}{\delta_w}. \tag{19}$$

It is possible to unambiguously define a *shell flux*,

$$\Psi_w(\theta,\phi)\equiv\psi(r_w,\theta,\phi), \tag{20}$$

in the thin shell limit, where

$$\psi(r,\theta,\phi)=\sum_{m,n}\psi^{m,n}(r)\,\mathrm{e}^{\,\mathrm{i}\,(m\,\theta-n\,\phi)}. \tag{21}$$

Let

$$\Psi_w(\theta,\phi)=\sum_{m,n}\Psi_w^{m,n}\,\mathrm{e}^{\,\mathrm{i}\,(m\,\theta-n\,\phi)}. \tag{22}$$

In the thin shell limit, the eddy currents induced in the shell have no significant radial variation. Hence, the radially integrated eddy current density can be written

$$\mu_0\,\delta\boldsymbol{I}_w=\mathrm{i}\,\nabla J_w\wedge\hat{\boldsymbol{r}}, \tag{23}$$

where $J_w(\theta,\phi)$ is the shell eddy current stream-function.

It is helpful to define the quantity

$$\Delta\Psi_w^{m,n} = \left[ r\,\frac{\partial\psi^{m,n}}{\partial r}\right]_{r_w-}^{r_w+}, \tag{24}$$

which parameterizes the jump in the radial derivative of $\psi^{m,n}$ across the shell. Ampère's law integrated across the shell yields

$$\Delta\Psi_w^{m,n} = -(m^2 + n^2\epsilon_w^2)\,J_w^{m,n}, \tag{25}$$

where

$$J_w(\theta,\phi) = \sum_{m,n} J_w^{m,n}\,\mathrm{e}^{\,\mathrm{i}\,(m\,\theta - n\,\phi)}, \tag{26}$$

and

$$\epsilon_w = \frac{r_w}{R_0}. \tag{27}$$

Ohm's law combined with Faraday's law yields

$$\Delta\Psi_w^{m,n} = \gamma\tau_w\,\Psi_w^{m,n}. \tag{28}$$

### D. The resistive shell mode

Equation (11) determines the flux function $\psi^{m,n}$ in the *outer region* (*i.e.*, everywhere apart from inside the shell). This equation is manifestly singular at the $m,n$ *rational flux surface*, where $(m\,B_\theta - n\epsilon\,B_\phi) = 0$, expect when this surface is situated in the vacuum region outside the plasma (where $\sigma' = 0$). A physically acceptable solution of Eq. (11) must satisfy physical boundary conditions at $r = 0$ and $r = \infty$, with $\psi^{m,n}$ continuous across the shell. In addition, $\psi^{m,n}$ must be zero at any $m,n$ rational surface lying inside the plasma. The latter constraint comes about because modes which interact strongly with the shell tend to rotate very slowly in the laboratory frame, and, therefore, do not reconnect magnetic flux inside the plasma, which is usually rotating substantially faster than the rate of resistive reconnection[10]. In general, there is a discontinuity in the radial derivative of $\psi^{m,n}$ at $r = r_w$. The *shell stability index*,

$$E_{ww}^{m,n} = \left[ r\,\frac{d\psi^{m,n}}{dr}\Big/\psi^{m,n}\right]_{r_w-}^{r_w+}, \tag{29}$$

is uniquely defined for every $m,n$ harmonic.

Asymptotic matching between the *inner region* (*i.e.*, the shell) and the *outer region* gives

$$\Delta\Psi_w^{m,n} = E_{ww}^{m,n}\,\Psi_w^{m,n}. \tag{30}$$

Equations (28) and (30) yield the standard dispersion relation for the $m,n$ resistive shell mode:

$$\gamma\tau_w = E_{ww}^{m,n}. \tag{31}$$

Clearly, this mode is unstable whenever $E_{ww}^{m,n} > 0$, and is stable otherwise.

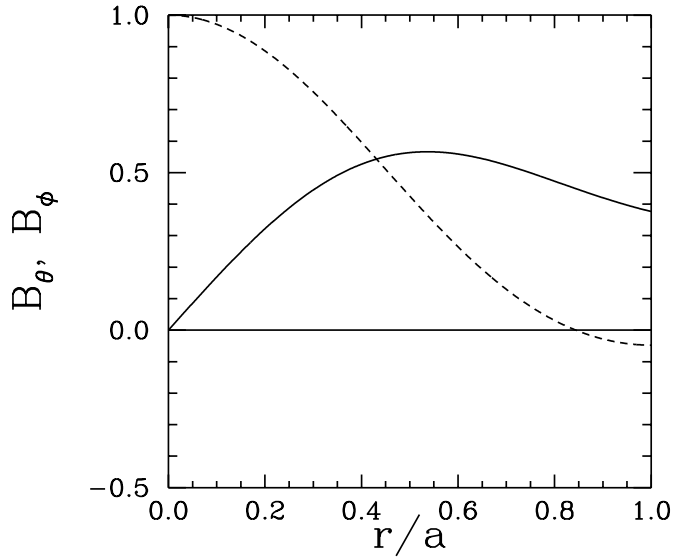


FIG. 1. The magnetic field associated with an RFP equilibrium characterized by $\epsilon_0 = 0.2$, $\alpha = 3$, $\Theta_0 = 1.71272$, $F = -0.2$, and $\Theta = 1.58696$. The solid line corresponds to $B_\theta$, whereas the dashed line corresponds to $B_\phi$. Both fields are normalized such that the on-axis toroidal field-strength is unity.

### E. Stability of the resistive shell mode

Consider an example RFP equilibrium for which $\epsilon_0 = 0.2$, $\alpha = 3$, $\Theta_0 = 1.71272$, $F = -0.2$, and $\Theta = 1.58696$. Here,

$$\epsilon_0 = \frac{a}{R_0} \tag{32}$$

is the inverse aspect-ratio of the plasma. Figure 1 shows the magnetic field associated with this equilibrium.

Suppose that the resistive shell is located right on the plasma boundary, so that $r_w = a$. In this case, the only unstable resistive shell modes are $m = 1$ modes with toroidal mode numbers lying in the range $n = -4$ to $+9$. Thus, there are 14 unstable resistive shell modes. Figure 2 shows the shell stability indices for these modes plotted as a function of $n\epsilon_0$. Of course, the equilibrium is also unstable to $m = 1$ tearing modes, resonant in the plasma core [31]. However, these tearing modes rotate with the plasma, and, therefore, do not penetrate the shell, or interact significantly with the slowly rotating resistive shell modes.

Note that, unlike a tokamak, where there is generally only *one* unstable resistive shell mode at any given time [24], a thin-shell RFP is characterized by the presence of *many* unstable resistive shell modes. In fact, the number of unstable modes is roughly proportional to the aspect-ratio, $R_0/a$, of the device. Thus, any feedback stabilization scheme for resistive shell modes in an RFP must be capable of *simultaneously stabilizing many unstable modes.*

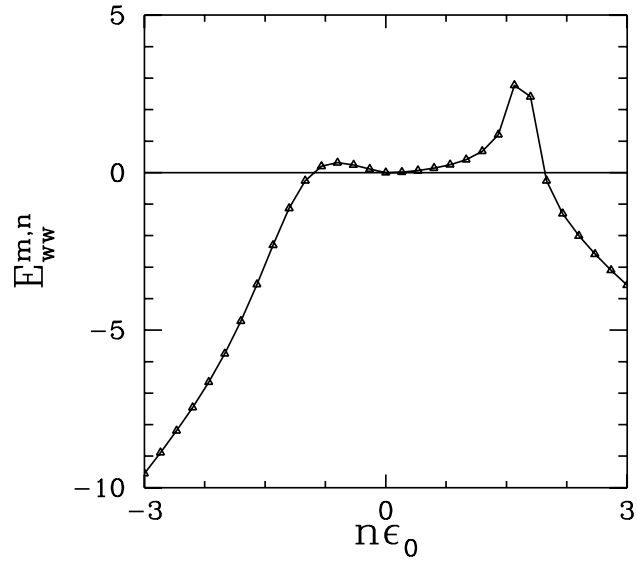


FIG. 2. The shell stability indices $E^{m,n}_{ww}$ for $m = 1$ resistive shell modes plotted as a function of $n\epsilon_0$ for an RFP equilibrium characterized by $\epsilon_0 = 0.2$, $\alpha = 3$, $\Theta_0 = 1.71272$, $F = -0.2$, and $\Theta = 1.58696$.

## III. THE FEEDBACK MODIFIED DISPERSION RELATION

### A. Introduction

Suppose that a set of feedback coils is installed outside the shell at minor radius $r_f$. The radially integrated current density carried by these coils is written

$$\mu_0\,\delta\boldsymbol{I}_f = \mathrm{i}\,\nabla J_f \wedge \hat{\boldsymbol{r}}, \tag{33}$$

where $J_f(\theta,\phi)$ is the feedback current stream-function. Let

$$J_f(\theta,\phi) = \sum_{m,n} J_f^{m,n}\,\mathrm{e}^{\,\mathrm{i}\,(m\,\theta - n\,\phi)}. \tag{34}$$

The *feedback flux* is defined

$$\Psi_f(\theta,\phi) \equiv \psi(r_f,\theta,\phi). \tag{35}$$

Let

$$\Psi_f(\theta,\phi) = \sum_{m,n} \Psi_f^{m,n}\,\mathrm{e}^{\,\mathrm{i}\,(m\,\theta - n\,\phi)}. \tag{36}$$

It is helpful to define the quantity

$$\Delta\Psi_f^{m,n} = \left[r\,\frac{\partial\psi^{m,n}}{\partial r}\right]_{r_f-}^{r_f+}, \tag{37}$$

which parameterizes the jump in the radial derivative of $\psi^{m,n}$ across the feedback coils.

Asymptotic matching in the vacuum region surrounding the plasma, making use of the general vacuum solution (14), yields the following feedback modified dispersion relation for the $m,n$ resistive shell mode:

$$\Delta\Psi_w^{m,n} = \left(E_{ww}^{m,n} + \frac{E_{wf}^{m,n}\,E_{fw}^{m,n}}{E_{ff}^{m,n}}\right)\Psi_w^{m,n} + E_{wf}^{m,n}\,\Psi_f^{m,n}, \tag{38}$$

$$\Delta\Psi_f^{m,n} = E_{ff}^{m,n}\,\Psi_f^{m,n} + E_{fw}^{m,n}\,\Psi_w^{m,n}. \tag{39}$$

Here,

$$E_{wf}^{m,n} = \frac{(m^2 + n^2\epsilon_w^2)}{i_m(n\epsilon_w)\, k_m(n\epsilon_f) - k_m(n\epsilon_w)\, i_m(n\epsilon_f)}, \tag{40}$$

$$E_{fw}^{m,n} = \frac{(m^2 + n^2\epsilon_f^2)}{i_m(n\epsilon_w)\, k_m(n\epsilon_f) - k_m(n\epsilon_w)\, i_m(n\epsilon_f)}, \tag{41}$$

$$E_{ff}^{m,n} = -\frac{k_m(n\epsilon_w)\,(m^2 + n^2\epsilon_f^2)}{k_m(n\epsilon_f)\,[i_m(n\epsilon_w)\, k_m(n\epsilon_f) - k_m(n\epsilon_w)\, i_m(n\epsilon_f)]}, \tag{42}$$

where

$$\epsilon_f = \frac{r_f}{R_0}. \tag{43}$$

For the special case $n = 0$,

$$E_{wf}^{m,n} = E_{fw}^{m,n} = \frac{2m\,(\epsilon_f/\epsilon_w)^m}{(\epsilon_f/\epsilon_w)^{2m} - 1}, \tag{44}$$

$$E_{ff}^{m,n} = -\frac{2m\,(\epsilon_f/\epsilon_w)^{2m}}{(\epsilon_f/\epsilon_w)^{2m} - 1}. \tag{45}$$

Equations (25) and (28) remain valid, so that

$$\Delta\Psi_w^{m,n} = -(m^2 + n^2\epsilon_w^2)\, J_w^{m,n} = \gamma\tau_w\, \Psi_w^{m,n}. \tag{46}$$

By direct analogy with Eq. (25),

$$\Delta\Psi_f^{m,n} = -(m^2 + n^2\epsilon_f^2)\, J_f^{m,n}. \tag{47}$$

Equations (38), (39), (46), and (47) can be rearranged to give

$$(m^2 + n^2\epsilon_f^2)\, J_f^{m,n} = -\frac{E_{ff}^{m,n}}{E_{wf}^{m,n}}\,(\gamma\tau_w - E_{ww}^{m,n})\, \Psi_w^{m,n}. \tag{48}$$

### B. The feedback coils

The distribution of feedback coils is assumed to be *poloidally symmetric*. It is further assumed that there are sufficient, closely spaced coils in the poloidal direction that there is *negligible coupling* of different poloidal harmonics by the feedback currents.

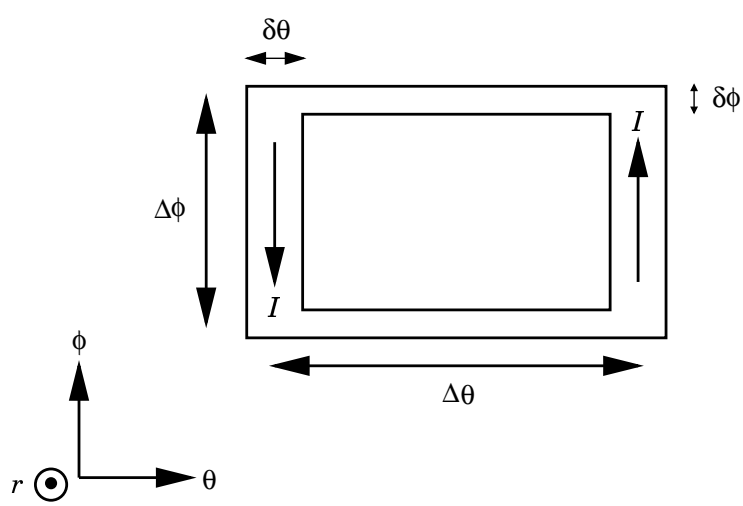


FIG. 3. An individual feedback coil

Suppose, for the sake of simplicity, that all of the feedback loops are identical, and consist of (radially) thin, rectangular, saddle coils, as illustrated in Fig. 3. The poloidal and toroidal angular extents of each coil are $\Delta\theta$ and $\Delta\phi$, respectively. Furthermore, the angular widths of the toroidal and poloidal legs of each coil are $\delta\theta$ and $\delta\phi$, respectively. Suppose that there are $N$ coils in the toroidal direction, with the $k$th coil centred on toroidal angle $\phi_k$.

Let $I_k$ be the total current circulating around the $k$th coil. For the sake of simplicity, this current is assumed to be *uniformly distributed* throughout the coil. It follows from Eq. (33) that

$$\mathrm{i}\,\frac{\partial J_f}{\partial\phi} = \begin{cases} -\mu_0 I_k/\delta\phi & \text{for } \phi_k + \Delta\phi/2 - \delta\phi/2 < \phi < \phi_k + \Delta\phi/2 + \delta\phi/2 \\ +\mu_0 I_k/\delta\phi & \text{for } \phi_k - \Delta\phi/2 - \delta\phi/2 < \phi < \phi_k - \Delta\phi/2 + \delta\phi/2 \\ 0 & \text{otherwise} \end{cases}, \tag{49}$$

where $k$ runs from 1 to $N$. Now,

$$J_f^{m,n} = -\oint \frac{\partial J_f}{\partial\phi}\,\frac{\mathrm{e}^{\,\mathrm{i}\,n\,\phi}}{\mathrm{i}\,n}\,\frac{d\phi}{2\pi}, \tag{50}$$

giving

$$\mathrm{i}\,J_f^{m,n} = \frac{2\,\mu_0}{\pi\,\delta\phi}\,\frac{\sin(n\delta\phi/2)\,\sin(n\Delta\phi/2)}{n^2}\sum_{k=1,N} I_k\,\mathrm{e}^{\,\mathrm{i}\,n\,\phi_k}. \tag{51}$$

Note that the common $\mathrm{e}^{\,\mathrm{i}\,m\,\theta}$ dependence of perturbed quantities has been neglected for ease of notation.

### C. The feedback algorithm

Suppose that each feedback coil is accompanied by an equal area detector loop, located at the same angular position, but the *shell radius*, which measures the perturbed magnetic flux leaking through the shell. The perturbed magnetic flux linking the $k$th detector loop is written

$$\Phi_k = \int_{k\text{th coil}} \boldsymbol{b}\cdot\hat{\boldsymbol{r}}\,dA = \mathrm{i}\,R_0\,\Delta\theta\int_{\phi_k-\Delta\phi/2}^{\phi_k+\Delta\phi/2}\sum_n \Psi_w^{m,n}\,\mathrm{e}^{-\mathrm{i}\,n\,\phi}\,d\phi. \tag{52}$$

It is easily demonstrated that

$$\Phi_k = 2\,\mathrm{i}\,R_0\,\Delta\theta\sum_n \frac{\sin(n\Delta\phi/2)}{n}\,\Psi_w^{m,n}\,\mathrm{e}^{-\mathrm{i}\,n\,\phi_k}. \tag{53}$$

The feedback algorithm adopted in this paper is very straightforward: the current driven around each feedback coil is *directly proportional* to minus the perturbed magnetic flux linking the associated detector loop. It follows that

$$\mu_0\,I_k = -Q_k\,\Phi_k, \tag{54}$$

where $Q_k$ is the *gain* in the $k$th feedback circuit.

### D. The dispersion relation

Equations (48), (51), (53), and (54) can be combined to give the dispersion relation

$$I_k = \hat{Q}_k\sum_n F^{m,n}(\gamma\tau_w)\sum_{k'=1,N}\frac{\mathrm{e}^{-\mathrm{i}\,n\,(\phi_k-\phi_{k'})}}{N}\,I_{k'}, \tag{55}$$

where

$$\hat{Q}_k = \frac{Q_k}{Q_0}, \tag{56}$$

for $k = 1$ to $N$. Here,

$$Q_0 = \frac{\pi\,\delta\phi}{4\,R_0\,\Delta\theta\,N\,\epsilon_w^3}, \tag{57}$$

$$\eta^{m,n} = -\frac{E_{wf}^{m,n}}{E_{ff}^{m,n}}\frac{m^2+n^2\epsilon_f^2}{m^2+n^2\epsilon_w^2} = \frac{k_m(n\epsilon_f)}{k_m(n\epsilon_w)}, \tag{58}$$

and

$$F^{m,n} = \frac{\eta^{m,n}}{E_{ww}^{m,n}-\gamma\tau_w}\frac{m^2+n^2\epsilon_w^2}{n^3\,\epsilon_w^3}\,\sin(n\delta\phi/2)\,\sin^2(n\Delta\phi/2). \tag{59}$$

For the special case $n = 0$,

$$\eta^{m,n} = \left(\frac{\epsilon_w}{\epsilon_f}\right)^m, \tag{60}$$

and $F^{m,n}$ is evaluated according to L'Hôpital's rule.

## IV. ANALYSIS OF AN $N$-FOLD TOROIDALLY SYMMETRIC FEEDBACK SCHEME

### A. Introduction

Consider a feedback scheme which possesses pure $N$-fold toroidal symmetry. In such a scheme, the feedback coils, and their associated detector loops, are *equally spaced* in the toroidal direction, so that

$$\phi_k = (k-1)\,\frac{2\pi}{N}, \tag{61}$$

for $k = 1$ to $N$. Likewise, the gains in all the feedback circuits are equal, so that

$$\hat{Q}_k = \hat{Q}, \tag{62}$$

for all $k$. In this case, it is easily demonstrated that

$$\sum_{k'=1,N}\frac{\mathrm{e}^{-\mathrm{i}\,l\,\phi_{k'}}\,\mathrm{e}^{-\mathrm{i}\,n\,(\phi_k-\phi_{k'})}}{N} = \begin{cases}\mathrm{e}^{-\mathrm{i}\,l\,\phi_k} & \text{if } n = l + j\,N\\ 0 & \text{otherwise}\end{cases}, \tag{63}$$

where $j$ is an integer.

The most general solution to the symmetrized dispersion relation is

$$I_k = \sum_{l=1,N}\mathcal{J}_l\,\mathrm{e}^{-\mathrm{i}\,l\,\phi_k}. \tag{64}$$

Substitution of the above into Eq. (55), making use of Eqs. (61)–(63), yields

$$\sum_{l=1,N}\mathcal{J}_l\,\mathrm{e}^{-\mathrm{i}\,l\,\phi_k} = \hat{Q}\sum_{l=1,N}\sigma_l(\gamma\tau_w)\,\mathcal{J}_l\,\mathrm{e}^{-\mathrm{i}\,l\,\phi_k}, \tag{65}$$

for $k = 1$ to $N$, where

$$\sigma_l = \sum_{j}^{n=l+j\,N} F^{m,n}. \tag{66}$$

It follows from Eq. (63) that the coefficients of $\mathrm{e}^{-\mathrm{i}\,l\,\phi_k}$, for different values of $l$, can be equated in (65). Thus,

$$\hat{Q}^{-1} = \sigma_l(\gamma\tau_w), \tag{67}$$

for $l = 1$ to $N$. In other words, the general dispersion relation (55) separates into $N$ independent subsidiary dispersion relations for an $N$-fold toroidally symmetric feedback scheme. Each of these subsidiary dispersion relations deals with a different set of toroidal harmonics coupled together by the feedback currents.

### B. Graphical solution of the $l$th subsidiary dispersion relation

Consider the $l$th subsidiary dispersion relation. It is convenient to label the toroidal mode numbers of the coupled harmonics as follows,

$$n_{0(l)}, n_{1(l)}, n_{2(l)}, \cdots, \tag{68}$$

where

$$E_{ww}^{m,n_{0(l)}} > E_{ww}^{m,n_{1(l)}} > E_{ww}^{m,n_{2(l)}} \cdots. \tag{69}$$

In other words, the $m, n_{0(l)}$ mode is the first most unstable harmonic, the $m, n_{1(1)}$ mode is the second most unstable harmonic, *etc.* Let

$$E_{ww}^{m,n_{j(l)}} \equiv E_{j(l)}, \tag{70}$$

for $j = 0, 1, 2, \cdots$.

Making use of the above definitions, the $l$th subsidiary dispersion relation can be written

$$\hat{Q}^{-1} = \sigma_l(\gamma\tau_w) = \sum_{j=0,1,2,\cdots} \frac{\eta^{m,n_{j(l)}}}{E_{j(l)} - \gamma\tau_w} \frac{[m^2 + (n_{j(l)}\epsilon_w)^2]}{[n_{j(l)}\,\epsilon_w]^3} \sin[n_{j(l)}\delta\phi/2]\,\sin^2[n_{j(l)}\,\Delta\phi/2]. \tag{71}$$

Note that $\eta^{m,n} > 0$ for all $m, n$. Likewise, $\delta\phi$ can be made sufficiently small that $\sin[n_{j(l)}\delta\phi/2] > 0$ for the first few coupled harmonics (*i.e.*, $m, n_{0(l)}$, $m, n_{1(l)}$, $m, n_{2(l)}$, *etc.*). It follows that the dispersion relation (71) can be represented schematically as shown in Fig. 4. The growth-rates of the various coupled modes are determined by the intercepts between a horizontal line of height $\hat{Q}^{-1}$ and the curve $\sigma_l(\gamma\tau_w)$. The unperturbed (*i.e.*, $\hat{Q} = 0$) growth-rates are determined by the infinities of $\sigma_l$, whereas the growth-rates in the presence of very strong feedback (*i.e.*, $\hat{Q} \to \infty$) are determined by the zeros of $\sigma_l$. More explicitly, the first most unstable mode moves from point $A$ on the diagram to point $B$, as the feedback gain is gradually increased from zero to a very large value, whereas the second most unstable mode moves from point $C$ to point $D$. It is clear from the diagram that the following inequality is satisfied for $j = 0, 1, \cdots$ and $0 \leq \hat{Q} < \infty$:

$$E_{j-1(l)} < \gamma_{j(l)}(\hat{Q})\,\tau_w \leq E_{j(l)}. \tag{72}$$

Here, $\gamma_{j(l)}(\hat{Q})$ is the growth-rate of the $j+1$ th most unstable mode when the normalized feedback gain is $\hat{Q}$. According to the above inequality, the feedback modified growth-rate of the $j+1$ th most unstable mode always lies between the unperturbed growth-rates of the $j+1$ th and $j+2$ th most unstable modes.

Two important caveats follow immediately from the inequality (72). Firstly, if *all* of the coupled modes are intrinsically stable (*i.e.*, $E_{0(l)} < 0$) then they all *remain stable* under the action of feedback (with $\hat{Q}$ in the range $0 \to \infty$). Secondly, if *more than one* of the coupled modes are intrinsically unstable (*i.e.*, $E_{1(l)} > 0$) then the feedback scheme is *incapable* of stabilizing all of the modes.

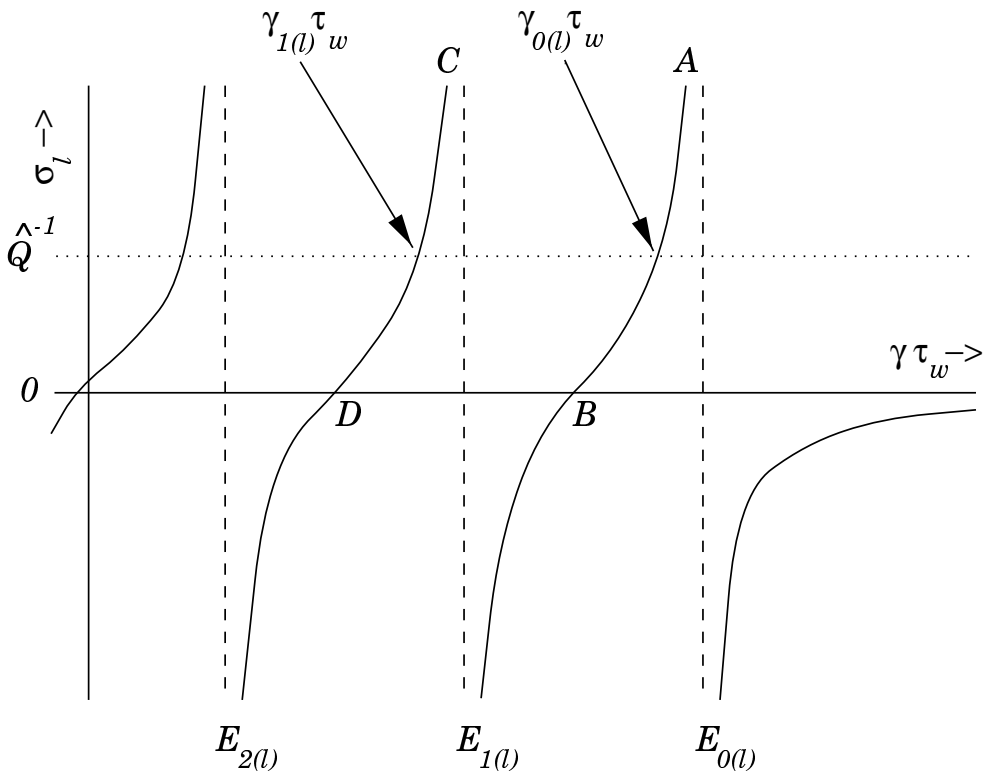


FIG. 4. A schematic diagram of the $l$th subsidiary dispersion relation.

### C. Stabilization criterion for the $l$th subsidiary dispersion relation

The only non-trivial situation in which the feedback scheme is capable of stabilizing all of the modes associated with the $l$th subsidiary dispersion relation is that where only one of these modes is intrinsically unstable: *i.e.*, $E_{0(l)} > 0$, and $E_{1(l)} < 0$. In this case, the dispersion relation (71) can be represented schematically as shown in Fig. 5. It can be seen that the feedback scheme is capable of stabilizing the $m, n_{0(l)}$ mode provided that

$$\sigma_l(0) > 0, \tag{73}$$

in which case the critical normalized gain above which stabilization is achieved is given by

$$\hat{Q}_{c(l)} = \frac{1}{\sigma_l(0)}. \tag{74}$$

Equation (71) and (73) can be combined to give the stabilization criterion

$$\alpha_l < 1, \tag{75}$$

where

$$\alpha_l = \sum_{j=1,2,3,\cdots} \frac{E_{0(l)}}{[-E_{j(l)}]} \frac{\eta^{m,n_{j(l)}}}{\eta^{m,n_{0(l)}}} \left(\frac{n_{0(l)}}{n_{j(l)}}\right)^3 \frac{[m^2 + (n_{j(l)}\epsilon_w)^2]}{[m^2 + (n_{0(l)}\epsilon_w)^2]} \frac{\sin[n_{j(l)}\delta\phi/2]\,\sin^2[n_{j(l)}\Delta\phi/2]}{\sin[n_{0(l)}\delta\phi/2]\,\sin^2[n_{0(l)}\Delta\phi/2]} \tag{76}$$

measures the feedback induced coupling between the intrinsically unstable $m, n_{0(l)}$ mode and the intrinsically stable $m, n_{j(l)}$ modes. According to Eq. (75), the feedback scheme is only capable of stabilizing the $m, n_{0(l)}$ mode provided that this coupling is *sufficiently weak*[24].

The critical value of $\hat{Q}$ above which the $m, n_{0(l)}$ mode is stabilized can be written

$$\hat{Q}_{c(l)} = \frac{E_{0(l)}}{\eta^{m,n_{0(l)}}} \frac{[n_{0(l)}\,\epsilon_w]^3}{[m^2 + (n_{0(l)}\epsilon_w)^2]} \frac{1}{\sin[n_{0(l)}\delta\phi/2]\,\sin^2[n_{0(l)}\Delta\phi/2]} \frac{1}{1-\alpha_l}. \tag{77}$$

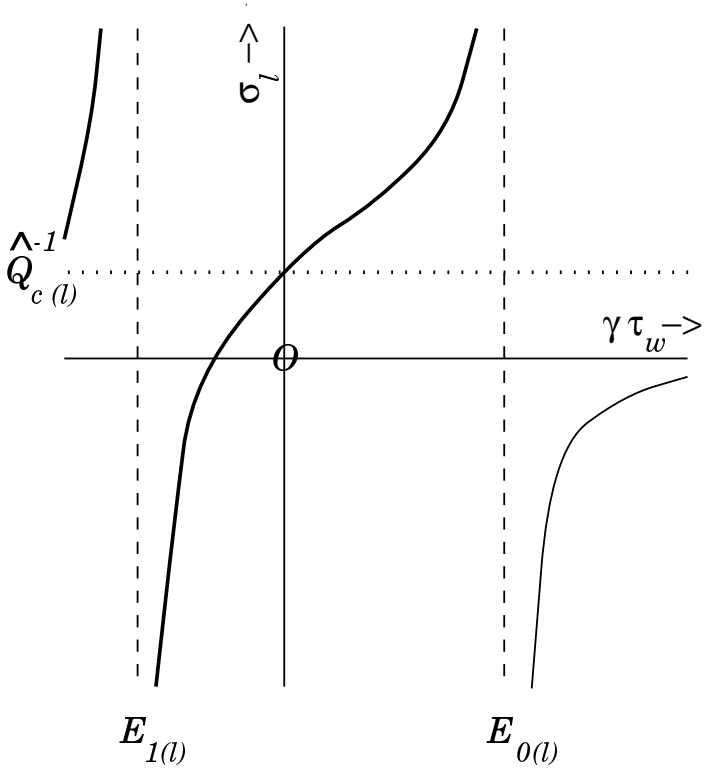


FIG. 5. A schematic diagram of the $l$th subsidiary dispersion relation for the case of a single intrinsically unstable mode.

### D. Approximate evaluation of the mode coupling parameter

The mode coupling parameter $\alpha_l$ can be evaluated approximately in the limit $N\epsilon_w \gg 1$, in which the toroidal mode numbers of the intrinsically stable harmonics satisfy

$$n_{j(l)}\epsilon_w \gg 1, \tag{78}$$

for $j = 1, 2, 3, \cdots$. In this case, it is easily demonstrated that

$$E_{j(l)} \simeq -2\,|n_{j(l)}|\,\epsilon_w, \tag{79}$$

and

$$\eta_{m,n_{j\,(l)}} \simeq \sqrt{\frac{r_f}{r_w}}\;\mathrm{e}^{-|n_{j(l)}|\,(\epsilon_f-\epsilon_w)}, \tag{80}$$

for the intrinsically stable harmonics. Thus, in the limit $\delta\phi \to 0$, Eq. (76) yields

$$\alpha_l \simeq \frac{E_{0(l)}}{N\epsilon_w}\,\frac{\sqrt{r_f/r_w}}{\eta^{m,n_{0\,(l)}}}\,\frac{[n_{0(l)}\epsilon_w]^2}{m^2+[n_{0(l)}\epsilon_w]^2}\,\frac{\beta_l}{\sin^2[n_{0(l)}\Delta\phi/2]}, \tag{81}$$

where

$$\beta_l = \sum_{j=1,\infty}\frac{\sin^2(j\,N\Delta\phi/2)}{j}\,\mathrm{e}^{-j\,N\,(\epsilon_f-\epsilon_w)}, \tag{82}$$

since $n_{j(l)} \simeq \pm j\,N$. It can be demonstrated that

$$\beta_l = \frac{1}{4}\,\ln\left[1+\frac{\sin^2(N\Delta\phi/2)}{\sinh^2\{N\,(\epsilon_f-\epsilon_w)/2\}}\right] \simeq \sin^2(N\Delta\phi/2)\,\mathrm{e}^{-N\,(\epsilon_f-\epsilon_w)}, \tag{83}$$

provided $N\,(\epsilon_f - \epsilon_w) \gg 1$. The above expression obviously generalizes to

$$\beta_l \simeq \sin^2(N\Delta\phi/2)\,\mathrm{sinc}(N\delta\phi/2)\,\mathrm{e}^{-N\,(\epsilon_f-\epsilon_w)}, \tag{84}$$

when $\delta\phi$ is small but non-zero. Here, $\mathrm{sinc}(x) \equiv \sin(x)/x$. Hence, the final expression for the mode coupling parameter is

$$\alpha_l \simeq \frac{E_{0(l)}}{N\epsilon_w}\,\frac{\sqrt{r_f/r_w}}{\eta^{m,n_{0(l)}}}\,\frac{[n_{0(l)}\epsilon_w]^2}{m^2+[n_{0(l)}\epsilon_w]^2}\,\frac{\sin^2(N\Delta\phi/2)\,\mathrm{sinc}(N\delta\phi/2)}{\sin^2[n_{0(l)}\Delta\phi/2]}\;\mathrm{e}^{-N\,(\epsilon_f-\epsilon_w)}. \tag{85}$$

### E. A strategy for feedback stabilization of resistive shell modes in an RFP

Suppose that the intrinsically unstable ($m = 1$) resistive shell modes possess toroidal mode numbers in the range $n_{\min}$ to $n_{\max}$ (where $n_{\max} \geq n_{\min}$). Let

$$\Delta n = n_{\max} - n_{\min} + 1. \tag{86}$$

Consider a pure $N$-fold toroidally symmetric feedback scheme. It is clear, from the above analysis, that if $N < \Delta n$ then the general dispersion relation separates into $N$ subsidiary dispersion relations, some of which couple *more than one* intrinsically unstable resistive shell mode. In this case, the feedback scheme is *incapable* of simultaneously stabilizing all of the unstable modes. On the other hand, if

$$N \geq \Delta n \tag{87}$$

then the general dispersion relation separates into $N$ subsidiary dispersion relations, each of which couples, at most, *a single* intrinsically unstable resistive shell mode. In this case, the feedback scheme is *capable* of simultaneously stabilizing all of the unstable modes. The stabilization criterion is that the mode coupling parameters $\alpha_l$ [see Eq. (76)] must be less than unity for all subsidiary dispersion relations.

According to the approximate formula (85), the mode coupling parameter $\alpha_l$ for the $l$th subsidiary dispersion relation generally increases as the intrinsically unstable $1, n_{0(l)}$ mode becomes more unstable (*i.e.*, as $E_{0(l)}$ increases), decreases as the number of coils $N$ increases, the angular thickness $\delta\phi$ of the poloidal legs of the feedback coils increases, or the radial spacing $r_f - r_w$ between the feedback coils and the detector loops increases, and is a complicated function of the toroidal angular width $\Delta\phi$ of the feedback coils.

It follows, from the above discussion, that an appropriate strategy for the simultaneous feedback stabilization of all intrinsically unstable resistive shell modes in an RFP is to employ an $N$-fold toroidally symmetric feedback scheme, taking care to ensure that the number of coils in the toroidal direction $N$ is always greater than, or equal to, the range of toroidal mode numbers $\Delta n$ of the intrinsically unstable modes. Note that, even when $N \geq \Delta n$, the feedback scheme can be defeated by excessive mode coupling due to the non-sinusoidal nature of the feedback currents. This mode coupling can be minimized (at least, in the large $N$ limit) by increasing the number of feedback coils $N$, increasing the angular thickness $\delta\phi$ of the poloidal legs of the feedback coils, or increasing the radial spacing $r_f - r_w$ between the feedback coils and the detector loops.

## V. FEEDBACK COIL DESIGN

### A. Introduction

Consider the example RFP equilibrium illustrated in Fig. 1. As shown in Fig. 2, the intrinsically unstable ($m = 1$) resistive shell modes possess toroidal mode numbers lying in the range $n_{\min} = -4$ to $n_{\max} = 9$, so that $\Delta n = 14$. According to the previous analysis, it is, in principal, possible to simultaneously stabilize all of these modes using a 14-fold (*i.e.*, $N = 14$) toroidally symmetric feedback scheme. In practice, numerical solution of the feedback modified resistive shell mode dispersion relation (67) reveals that somewhat more than 14 coils in the toroidal direction are required to overcome the detrimental effects of feedback induced mode coupling. The smallest number of coils for which the feedback scheme is capable of operating successfully is 18 (*i.e.*, $N = 18$). In the following, a more optimal scheme is investigated which employs 20 coils in the toroidal direction (*i.e.*, $N = 20$).

### B. Coil design for a 20-fold toroidally symmetric feedback scheme

Consider the effect of a 20-fold (*i.e.*, $N = 20$) toroidally symmetric feedback scheme on the RFP equilibrium illustrated in Fig. 1. Note that none of the intrinsically unstable resistive shell modes are coupled together by the feedback scheme, so each intrinsically unstable mode can be treated as a *separate case*. Numerical solution of the feedback modified dispersion relation (67) reveals that the most difficult resistive shell modes to stabilize are the two most intrinsically unstable modes: *i.e.*, the $1,8$ and $1,9$ modes.

Figure 6 shows the critical normalized feedback gains $\hat{Q}_c$ required to stabilize the $1,8$ and $1,9$ modes plotted as functions of the angular width $\Delta\phi$ of the feedback coils, for $\delta\phi = 5°$, $r_w = 1.0\,a$, and $r_f = 1.1\,a$. The critical normalized feedback gains required to stabilize the other intrinsically unstable resistive shell modes are significantly smaller than those shown in Fig. 6. It can be seen that the optimum value of $\Delta\phi$ (*i.e.*, the value at which the critical gain required to simultaneously stabilize the $1,8$ and $1,9$ modes is minimized) is $23°$. This value corresponds to *overlapping* feedback coils in the toroidal direction[24].

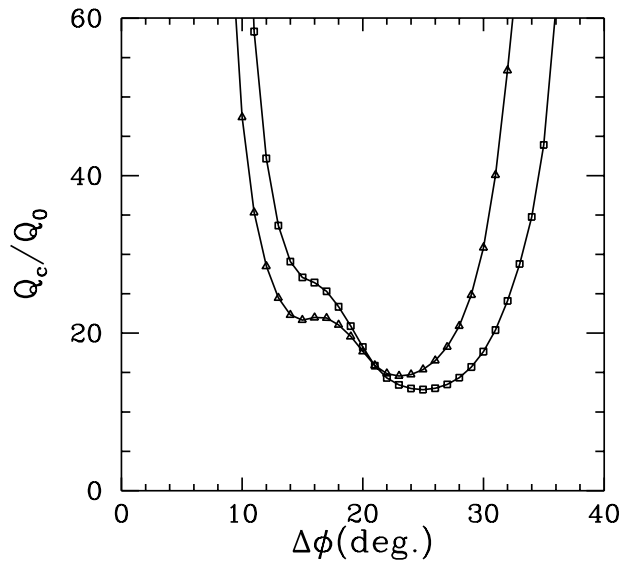


FIG. 6. The critical normalized feedback gain required to stabilize the $1,9$ ($\triangle$) and $1,8$ ($\square$) resistive shell modes as functions of the toroidal angular width $\Delta\phi$ of the feedback coils, calculated for $N = 20$, $\delta\phi = 5°$, $r_w = 1.0\,a$, and $r_f = 1.1\,a$.

Figure 7 shows the critical normalized feedback gain $\hat{Q}_c$ required to stabilize the $1,9$ resistive shell mode plotted as a function of the angular thickness $\delta\phi$ of the poloidal legs of the feedback coils, for $\Delta\phi = 23°$, $r_w = 1.0\,a$, and $r_f = 1.1\,a$. It can be seen that the critical gain at first decreases rapidly as $\delta\phi$ increases, and then levels off for $\delta\phi > 5°$. This behaviour is in accordance with the approximate formula (85), which predicts that the feedback induced mode coupling [and, hence, $\hat{Q}_c$—see Eq. (77)] should be a decreasing function of the coil thickness parameter $\delta\phi$. For practical reasons, it is desirable to minimize $\delta\phi$, in order to make the feedback coils as compact as possible. Thus, $\delta\phi = 5°$ is probably the optimum thickness of the feedback coils, since this is approximately the smallest value of $\delta\phi$ for which the feedback scheme performs efficiently.

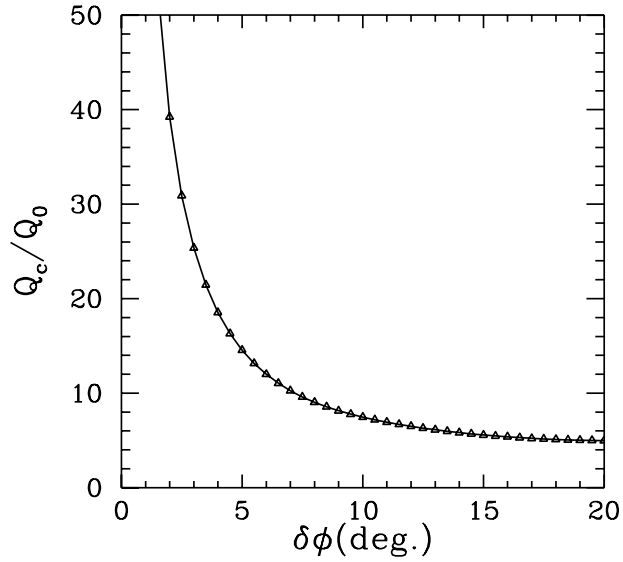


FIG. 7. The critical normalized feedback gain required to stabilize the $1,9$ resistive shell mode as a function of the angular thickness $\delta\phi$ of the poloidal legs of the feedback coils, calculated for $N = 20$, $\Delta\phi = 23°$, $r_w = 1.0\,a$, and $r_f = 1.1\,a$.

Figure 8 shows the critical normalized feedback gain $\hat{Q}_c$ required to stabilize the $1,9$ resistive shell mode plotted as a function of the minor radius $r_f$ of the feedback coil array, for $\Delta\phi = 23°$, $\delta\phi = 5°$, and $r_w = 1.0\,a$. It can be seen that the critical gain is a weakly increasing function of $r_f$. This behaviour *is not* in accordance with the approximate formula (85), which predicts that the feedback induced mode coupling [and, hence, $\hat{Q}_c$—see Eq. (77)] should be a decreasing function of the coil radius parameter $r_f$. It turns out that the latter scaling is only obtained in the extreme high-$N$ limit, where $N \gg \Delta n$. At moderate $N$-values, where $N \sim \Delta n$, the efficiency of the feedback scheme does not depend crucially on the radius of the feedback coil array. Thus, the choice $r_f = 1.1\,r_w$ is a reasonable one.

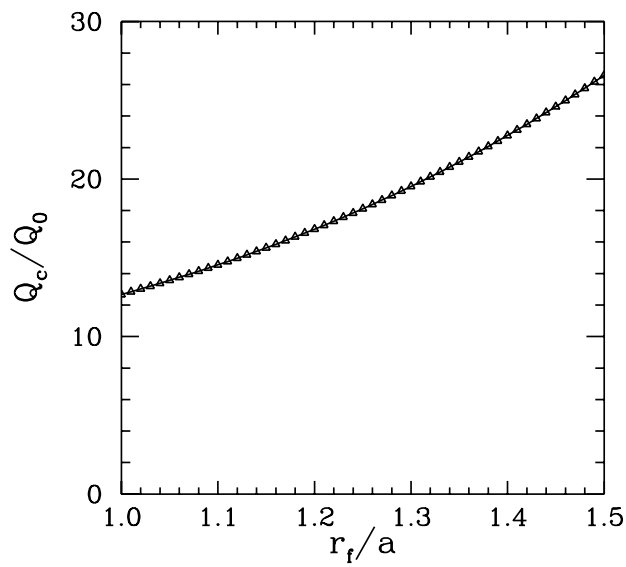


FIG. 8. The critical normalized feedback gain required to stabilize the $1,9$ resistive shell mode as a function of the minor radius $r_f$ of the feedback coil array, calculated for $N = 20$, $\Delta\phi = 23°$, $\delta\phi = 5°$, and $r_w = 1.0\,a$.

Figure 9 shows the critical normalized feedback gain $\hat{Q}_c$ required to stabilize the $1,9$ resistive shell mode plotted as a function of the shell minor radius $r_w$, for $\Delta\phi = 23°$, $\delta\phi = 5°$, and $r_f = 1.1\,r_w$. It can be seen that the critical gain is a very strongly increasing function of $r_w$. This behaviour is a consequence of the well-known fact that the intrinsic stability of resistive shell modes in an RFP rapidly worsens as the shell is moved away from the plasma edge. It is clear that the feedback scheme is only capable of operating successfully if the resistive shell is located *very close* to the edge of the plasma (*i.e.*, $r_w < 1.1\,a$).

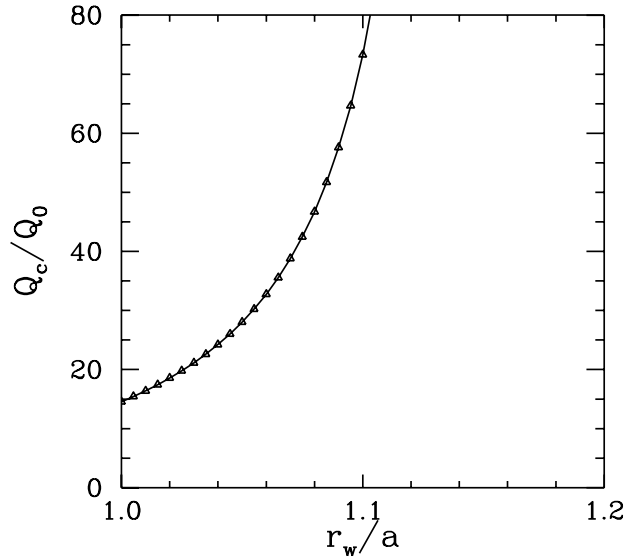


FIG. 9. The critical normalized feedback gain required to stabilize the $1,9$ resistive shell mode as a function of the shell minor radius $r_w$, calculated for $N = 20$, $\Delta\phi = 23°$, $\delta\phi = 5°$, and $r_f = 1.1\,r_w$.

In conclusion, a 20-fold toroidally symmetric feedback scheme is capable of simultaneously stabilizing all of the intrinsically unstable resistive shell modes associated with the RFP equilibrium illustrated in Fig. 1, provided that the shell is situated sufficiently close to the edge of the plasma (*i.e.*, $r_w < 1.1\,a$). The optimum toroidal angular width of the feedback coils is $\Delta\phi = 23°$, which corresponds to a configuration in which each coil *overlaps* its immediate neighbours in the toroidal direction[24]. The optimum angular thickness of the poloidal legs of the feedback coils is $\delta\phi = 5°$. Finally, the optimum minor radius of the feedback coil array is $r_f = 1.1\,r_w$.

### C. Robustness of the design

In the above, it is demonstrated that a 20-fold toroidally symmetric feedback scheme with the following parameters: $\Delta\phi = 23°$, $\delta\phi = 5°$, $r_w = 1.0\,a$, $r_f = 1.1\,a$: is capable of simultaneously stabilizing all of the intrinsically unstable resistive shell modes associated with a specific RFP equilibrium characterized by $\epsilon_0 = 0.2$, $\alpha = 3$, and $F = -0.2$ (see Fig. 1). In this section, the performance of the chosen feedback scheme is gauged against a wide range of RFP equilibria. As discussed previously, the requisite number of feedback coils in the toroidal direction is largely determined by the range of toroidal mode numbers $\Delta n$ of the intrinsically unstable resistive shell modes. In Tab. I this range is tabulated against the current peakedness parameter $\alpha$ and the reversal parameter $F$ for a set of RFP equilibria characterized by $\epsilon_0 = 0.2$ and $r_w = 1.0\,a$. Note that $\Delta n$ exhibits *very little variation* with $\alpha$ and $F$, as these parameters vary over the range of values typically encountered in RFP experiments. In fact, $\Delta n$ is largely determined by the inverse aspect-ratio $\epsilon_0$ of the equilibrium (broadly speaking, $\Delta n \propto 1/\epsilon_0$). It follows that it should be possible to design a feedback system which is capable of simultaneously stabilizing all intrinsically unstable resistive shell modes for a wide range of different values of the profile parameters $\alpha$ and $F$. As an illustration of this point, in Tab. I those values of $\Delta n$ (at fixed $\alpha$ and $F$) for which the previously mentioned feedback scheme *is not* capable of stabilizing all intrinsically unstable resistive shell modes are marked with an asterisk. It can be seen that the feedback scheme operates successfully over a wide range of different values of $\alpha$ and $F$. In fact, the feedback scheme only fails when the plasma current becomes too peaked (*i.e.*, $\alpha$ becomes too small), and the equilibrium consequently approaches too closely to the ideal stability boundary for one of the intrinsically unstable resistive shell modes.

It is concluded that, once the inverse aspect-ratio of the RFP is specified, it is relatively straightforward to design a feedback scheme capable of simultaneously stabilizing all intrinsically unstable resistive shell modes over a wide range of different plasma current profiles.

### D. The critical current

The critical current $I_c$ which must flow around each feedback coil in order to simultaneously stabilize all intrinsically unstable resistive shell modes is written

$$\frac{I_c}{I_\phi} \simeq \hat{Q}_c \, \frac{\delta\phi \, \Delta\phi}{8 \, N \, \epsilon_w^3} \, \frac{r_w}{a} \, \frac{b_r}{B_\theta(a)}, \tag{88}$$

where $\hat{Q}_c$ is the critical normalized feedback gain, $I_\phi$ is the equilibrium toroidal plasma current, and $b_r$ is the strength of the $m = 1$ radial magnetic field penetrating the shell. For the present design ($\hat{Q}_c \simeq 15$, $\delta\phi = 5^\circ$, $\Delta\phi = 23^\circ$, $N = 20$, $r_w = a$, $\epsilon_w = 0.2$), the above expression reduces to

$$\frac{I_c}{I_\phi} \simeq 0.41 \, \frac{b_r}{B_\theta(a)}. \tag{89}$$

Since $b_r$ is typically 1% of the equilibrium magnetic field-strength in RFPs, it follows that the typical current which must circulate around each feedback coil in order to stabilize all of the resistive shell modes is of order 1% of the equilibrium toroidal plasma current.

| | $\alpha$ | 2.2 | 2.3 | 2.4 | 2.5 | 2.6 | 2.7 | 2.8 | 2.9 | 3.0 | 3.1 | 3.2 | 3.3 | 3.4 | 3.5 | 3.6 | 3.7 | 3.8 | 3.9 | 4.0 | 4.5 | 5.0 | 10.0 |
|---|---|---|---|---|---|---|---|---|---|---|---|---|---|---|---|---|---|---|---|---|---|---|---|
| $F$ | | | | | | | | | | | | | | | | | | | | | | | |
| -0.5 | | – | 16* | 16* | 16 | 16 | 15 | 15 | 15 | 15 | 15 | 15 | 15 | 15 | 14 | 14 | 14 | 14 | 14 | 14 | 14 | 6 | 5 |
| -0.4 | | – | 16* | 16* | 16* | 16* | 16* | 15* | 15 | 15 | 15 | 15 | 15 | 15 | 15 | 14 | 14 | 14 | 14 | 14 | 13 | 13 | 5 |
| -0.3 | | – | – | – | – | – | 15* | 14* | 14 | 14 | 14 | 14 | 14 | 14 | 14 | 14 | 13 | 13 | 13 | 13 | 13 | 13 | 5 |
| -0.2 | | – | – | – | – | – | 15* | 15 | 14 | 14 | 14 | 14 | 14 | 14 | 14 | 14 | 14 | 14 | 13 | 13 | 13 | 13 | 12 |
| -0.1 | | – | – | – | – | – | 15* | 15 | 15 | 15 | 14 | 14 | 14 | 14 | 14 | 14 | 14 | 14 | 14 | 14 | 12 | 12 | 11 |
| 0.0 | | – | – | – | – | 15* | 14* | 14* | 14* | 14* | 14* | 14 | 14 | 14 | 14 | 13 | 13 | 13 | 13 | 13 | 13 | 13 | 12 |

TABLE I. The range of toroidal mode numbers $\Delta n$ of the ($m = 1$) intrinsically unstable resistive shell modes tabulated against the current peakedness parameter $\alpha$ and the reversal parameter $F$ for a set of RFP equilibria characterized by $\epsilon_0 = 0.2$ and $r_w = 1.0\,a$. A dash indicates that one or more of the resistive shell modes is ideally unstable. An asterisk indicates that the feedback scheme discussed in Sect. V is incapable of simultaneously stabilizing all of the modes.

## VI. EFFECT OF TOROIDAL ASYMMETRIES

### A. Introduction

The feedback scheme outlined in Sects. IV and V depends crucially for its successful operation on two factors. Firstly, the assumed pure $N$-fold toroidal *symmetry* of the scheme, and, secondly, the assumed pure *linear* response of the feedback circuits to the signals picked up by the detector loops. These factors permit the general resistive shell mode dispersion relation (55) to be split into $N$ *independent* subsidiary dispersion relations (67), each of which involves, at most, a single intrinsically unstable mode. Since, by definition, an RFP possesses a high degree of toroidal symmetry, it is plausible that a feedback system possessing almost pure $N$-fold toroidal symmetry could be installed outside the shell. Likewise, since the signals picked up by the detector loops only vary on the L/R time of the shell (because the signals must diffuse through the shell in order to be detected), and since the currents circulating in the feedback coils are relatively low [see Eq. (89)], it is also plausible that the feedback circuits could be constituted in such a manner that they exhibit an almost linear response. Nevertheless, in practice, there are always going to be small deviations from pure $N$-fold toroidal symmetry (generated, for instance, by the gaps in the shell) and pure linear response. These deviations give rise to *coupling* between the $N$ subsidiary dispersion relations. This section investigates the effect of such coupling on the operation of the feedback scheme.

### B. General analysis

The general resistive shell mode dispersion relation (55) can be rewritten

$$J_k = \sum_n F^{m,n}(\gamma\tau_w) \sum_{k'=1,N} \frac{\mathrm{e}^{-\mathrm{i}\,n\,(\phi_k-\phi_{k'})}}{N}\,\hat{Q}_{k'}\,J_{k'}\,, \tag{90}$$

for $k = 1$ to $N$, where

$$J_k = \frac{I_k}{\hat{Q}_k}. \tag{91}$$

A slight lack of pure $N$-fold symmetry in the feedback scheme, or a modest departure from pure linear response in the feedback circuits, can be modeled as a small sinusoidal toroidal variation in the gains of the various feedback circuits. Thus,

$$\hat{Q}_k = \hat{Q}\,[1 + 2\,\epsilon\,\cos(\Delta l\,\phi_k)]\,, \tag{92}$$

for $k = 1$ to $N$, where $\Delta l$ is an integer, and $\epsilon \ll 1$.

Let

$$J_k = \sum_{l=1,N} \mathcal{J}_l\,\mathrm{e}^{-\mathrm{i}\,l\,\phi_k}, \tag{93}$$

for $k = 1$ to $N$. Equation (90) reduces to

$$(\hat{Q}^{-1} - \sigma_l)\,\mathcal{J}_l = \epsilon\,\sigma_l\,(\mathcal{J}_{l+\Delta l} + \mathcal{J}_{l-\Delta l})\,, \tag{94}$$

for $l = 1$ to $N$. Here, use has been made of Eq. (63). Note that $\mathcal{J}_{l+j\,N} \equiv \mathcal{J}_l$, where $j$ is any integer. The above expression demonstrates how symmetry breaking effects (*i.e.*, $\epsilon \neq 0$) give rise to coupling between the subsidiary dispersion relations (*i.e.*, coupling between the $\mathcal{J}_l$ for different values of $l$).

### C. Coupling between the $l$th and $l'$th subsidiary dispersion relations

Suppose, for the sake of simplicity, that the dominant coupling is that between the $l$th and $l'$th subsidiary dispersion relations. In this case, Eq. (94) yields

$$(\hat{Q}^{-1} - \sigma_l)(\hat{Q}^{-1} - \sigma_{l'}) - \epsilon^2\,\sigma_l\,\sigma_{l'} = 0. \tag{95}$$

Of course, in the absence of any symmetry breaking effects (*i.e.*, $\epsilon = 0$), the two dispersion relations completely decouple from one another, giving $\hat{Q}^{-1} = \sigma_l$ and $\hat{Q}^{-1} = \sigma_{l'}$, independently. On the other hand, when $\epsilon = 1$ the two dispersion relations combine to give

$$\hat{Q}^{-1} = \sigma_l + \sigma_{l'}. \tag{96}$$

This expression is of the form (67), except that it couples all the toroidal harmonics associated with both the $l$th and $l'$th subsidiary dispersion relations. If the $l$th and $l'$th subsidiary dispersion relations each only involve a single intrinsically unstable harmonic, then Eq. (96) takes the form of a subsidiary dispersion relation involving two intrinsically unstable harmonics. According to the analysis of Sect. IV, these two harmonics cannot be simultaneously stabilized by the feedback scheme. It follows that if the symmetry breaking parameter $\epsilon$ is $O(1)$ then the coupling between the $l$th and $l'$th subsidiary dispersion relations is strong enough to defeat the feedback scheme.

Suppose that the symmetry breaking parameter $\epsilon$ is non-zero, but much less than unity. In this case, the modified $l$th subsidiary dispersion relation takes the form

$$\hat{Q}^{-1} = \sigma_l(\gamma\tau_w) + \epsilon^2\,\frac{\sigma_l(\gamma\tau_w)\,\sigma_{l'}(\gamma\tau_w)}{\hat{Q}^{-1} - \sigma_{l'}(\gamma\tau_w)}. \tag{97}$$

Clearly, for most values of the normalized feedback gain, $\hat{Q}$, the dispersion relation is only modified by a small factor of $O(\epsilon^2)$. In other words, a small amount of symmetry breaking has little effect on the $l$th subsidiary dispersion relation. Likewise, for the $l'$th subsidiary dispersion relation. The only exception to this rule occurs at a point in $\hat{Q}$-$\gamma\tau_w$ space where $\hat{Q}^{-1} - \sigma_l(\gamma\tau_w)$ and $\hat{Q}^{-1} - \sigma_{l'}(\gamma\tau_w)$ are small simultaneously: *i.e.*, a point where a root of the $l$th subsidiary dispersion relation crosses a root of the $l'$th dispersion relation.

Suppose that a root of the $l$th subsidiary dispersion relation crosses a root of the $l'$th dispersion relation at $\hat{Q} = \hat{Q}_0$ and $\gamma = \gamma_0$. It follows that in the immediate vicinity of the crossing point:

$$\sigma_l(\gamma\tau_w) = (\hat{Q}_0)^{-1} + \alpha\,(\gamma - \gamma_0)\,\tau_w, \tag{98}$$

$$\sigma_{l'}(\gamma\tau_w) = (\hat{Q}_0)^{-1} + \alpha'\,(\gamma - \gamma_0)\,\tau_w, \tag{99}$$

where $\alpha$ and $\alpha'$ are constants. Let

$$q = (\hat{Q})^{-1} - (\hat{Q}_0)^{-1}, \tag{100}$$

$$g = (\gamma - \gamma_0)\,\tau_w. \tag{101}$$

The solution to the coupled dispersion relation (95) in the vicinity of the crossing point is

$$2\,q = (\alpha + \alpha')\,g \pm \sqrt{(\alpha - \alpha')^2\,g^2 + 4\,(\epsilon/\hat{Q}_0)^2}. \tag{102}$$

It can be seen that in the immediate vicinity of the crossing point the symmetry breaking effects gives rise to $O(\epsilon)$ modifications of the $l$th and $l'$th subsidiary dispersion relations which are such as to prevent the true roots from actually crossing.

### D. Conclusion

In conclusion, the feedback scheme outlined in Sects. IV and V is not unduly affected by *small* deviations from pure $N$-fold toroidal symmetry or a pure linear response of the feedback circuits. If the deviations are $O(\epsilon)$ then the modifications to the $N$ independent subsidiary dispersion relations derived in the ideal (*i.e.*, $\epsilon = 0$) limit are $O(\epsilon^2)$, except in situations where when two (or more) roots belonging to different dispersion relations approach one another closely, in which case the modifications are $O(\epsilon)$.

## VII. SUMMARY AND CONCLUSIONS

In order for the RFP concept to be regarded as reactor relevant, it is necessary to demonstrate that an RFP can operate successfully when surrounded by a close-fitting resistive shell whose L/R time is much *shorter* than the pulse length. Resonant modes are largely unaffected by the resistivity of the shell, provided that the plasma rotation rate

greatly exceeds the inverse L/R time of the shell, as is generally the case in a rotating plasma. Thus, by far the most straightforward strategy for preventing any degradation in the stability of resonant modes due to a resistive shell is to maintain the plasma rotation[6]. It may be necessary to install an auxiliary momentum source, such as a neutral beam injector, to overcome the rotation breaking effect of non-axisymmetric eddy currents induced in the shell by rotating dynamo modes.

Non-resonant modes cannot be stabilized by plasma rotation, except in the unlikely event that the rotation becomes Alfvénic, and are, therefore, expected to manifest themselves as non-rotating *resistive shell modes*, growing on the L/R time of the shell. A general RFP equilibrium is expected to be unstable to many different resistive shell modes at the same time. These modes must be stabilized in an RFP reactor. The only viable stabilization mechanism is some form of *active feedback*.

In Sects. II and III, a feedback modified dispersion relation is derived for resistive shell modes in a large aspect-ratio, zero-$\beta$, RFP equilibrium. The feedback coils are assumed to be identical, thin saddle-loops located outside the shell. The detector loops have the same area as the feedback coils, but are located at the shell radius. Each feedback coil has an associated detector loop at the same angular position. The feedback algorithm is simply that the current driven around a given feedback coil is *directly proportional* to minus the perturbed magnetic flux measured by its associated detector loop.

In Sect. IV, it is demonstrated that an $N$-fold toroidally symmetric feedback scheme (*i.e.*, a feedback scheme with $N$ equally spaced coils in the toroidal direction, and with identical gains in all feedback circuits) is capable of *simultaneously stabilizing* all intrinsically unstable resistive shell modes in a typical RFP equilibrium. Three stabilization criteria must be satisfied in order for the feedback scheme to operate successfully. Firstly, the number of coils in the toroidal direction $N$ must be greater than, or equal to, the range of toroidal mode numbers $\Delta n$ of the intrinsically unstable resistive shell modes. Secondly, the coupling of different toroidal harmonics due to the non-sinusoidal nature of the feedback currents must not be too strong. Finally, the shell must be located relatively close to the edge of the plasma (*i.e.*, $r_w < 1.1\,a$).

The deleterious effects of feedback induced mode coupling can be minimized by *optimizing* the number, size, shape, and positions of the feedback coils. The optimization process is outlined in Sect. V. The optimum coil size is such that a given feedback coil overlaps its immediate neighbours in the toroidal direction.

As discussed in Sect. V, the range of toroidal mode numbers $\Delta n$ of the intrinsically unstable resistive shell modes is largely determined by the aspect-ratio of the plasma. This allows the design of a feedback scheme capable of simultaneously stabilizing all intrinsically unstable resistive shell modes over a *wide range* of different plasma current profiles.

At first sight, the feedback scheme discussed in this paper appears to depend crucially for its successful operation on its pure $N$-fold toroidal symmetry, and the assumed pure linear response of the feedback circuits. In Sect. VI, however, it is demonstrated that the feedback scheme is robust to *small* departures from pure $N$-fold toroidal symmetry and pure linear response. Moreover, the critical current which must be driven around the feedback coils in order to stabilize all the resistive shell modes is only of order 1% of the equilibrium toroidal plasma current. Thus, the feedback scheme appears eminently realizable experimentally.

This paper neglects the effects of non-linear coupling between dynamo and resistive shell modes. Indeed, this coupling is expected to be weak in a rotating plasma, because the dynamo modes are forced to propagate whereas the resistive shell modes remain stationary in the laboratory frame. The non-linear coupling between resistive shell modes of different helicities is also neglected in this paper. This coupling is mediated by the reversal surface[31]. However, if the plasma at the reversal surface is rotating, as is expected in a rotating plasma, then any non-linear coupling between stationary resistive shell modes of different helicities is strongly inhibited. Thus, it is plausible that the feedback scheme can prevent the amplitudes of the various resistive shell modes from becoming large enough for non-linear coupling to play an important role.

## ACKNOWLEDGMENTS

This research was funded by the U.S. Department of Energy under contracts DE-FG05-96ER-54346 and DE-FG03-98ER-54504.

---

[1] J.A. Wesson, and D.J. Campbell, "*Tokamaks*," 2nd Edition, (Clarenden Press, Oxford, England, 1998).

[2] H.A.B. Bodin, Nucl. Fusion **30**, 1717 (1990).
[3] J.B. Taylor, Phys. Rev. Lett. **33**, 1139 (1974).
[4] D.C. Robinson, Nucl. Fusion **18**, 939 (1978).
[5] Y.L. Ho, and S.C. Prager, Phys. Fluids **31**, 1673 (1988).
[6] Z.X. Jiang, A. Bondeson, and R. Paccagnella, Phys. Plasmas **2**, 442 (1995).
[7] S. Ortolani, and D.D. Schnack, "*Magnetohydrodynamics of plasma relaxation*," (World Scientific, Singapore, 1993).
[8] M.F.F. Nave, and J.A. Wesson, Nucl. Fusion **30**, 2575 (1990).
[9] T.C. Hender, C.G. Gimblett, and D.C. Robinson, Nucl. Fusion **29**, 1279 (1989).
[10] R. Fitzpatrick, Nucl. Fusion **33**, 1049 (1993).
[11] J.P. Goedbloed, D. Pfirsch, and H. Tasso, Nucl. Fusion **12**, 649 (1972).
[12] M. Tanaka, T. Tuda, and T. Takeda, Nucl. Fusion **13**, 199 (1973).
[13] T. Sometani, and K. Fukagawa, Jpn. J. Appl. Phys. **17**, 2035 (1978).
[14] G.F. Nalesso, and S. Costa, Nucl. Fusion **20**, 443 (1980).
[15] J.P. Friedberg, private communication (1995).
[16] T. Tamano, *et al.*, Phys. Rev. Lett. **59**, 1444 (1987).
[17] B. Alper, *et al.*, Plasma Phys. Contrld. Fusion **31**, 205 (1989).
[18] P. Brunsell, J.R. Drake, S. Mazur, and P. Nordlund, Physica Scripta **44**, 358 (1991).
[19] P. Greene, and S. Robertson, Phys. Fluids B **5**, 556 (1993).
[20] J. Drake, private communication (1998).
[21] C.M. Bishop, Plasma Phys. Contrld. Fusion **31**, 1179 (1994).
[22] R. Fitzpatrick, and T.H. Jensen, Phys. Plasmas **3**, 2641 (1996).
[23] R. Fitzpatrick, Phys. Plasmas **4**, 2519 (1997).
[24] R. Fitzpatrick, and E.P. Yu, Phys. Plasmas **5**, 2340 (1998).
[25] B. Alper, Phys. Fluids B **2**, 1338 (1990).
[26] E.J. Zita, S.C. Prager, Y.L. Ho, and D.D. Schnack, Nucl. Fusion **32**, 1941 (1992).
[27] The standard large aspect-ratio ordering is $R_0/a \gg 1$, where $R_0$ and $a$ are the major and minor radii of the plasma, respectively.
[28] The conventional definition of this parameter is $\beta = 2\mu_0\langle p\rangle/\langle B^2\rangle$, where $\langle\cdots\rangle$ denotes a volume average, $p$ is the plasma pressure, and $B$ is the magnetic field-strength.
[29] V. Antoni, D. Merlin, S. Ortolani, and R. Paccagnella, Nucl. Fusion **26**, 1711 (1986).
[30] W.A. Newcomb, Ann. Phys. **10**, 232 (1960).
[31] R. Fitzpatrick, "*Formation and locking of the slinky mode in reversed field pinches*," submitted to Physics of Plasmas.